Université Grenoble Alpes

Report

Mid-therm

MIRA Anna

Supervisors:
Yohan Payan, TIMC-IMAG Lab, CNRS & Univ. Grenoble Alpes
Serge Muller, GE-Healthcare, France
Ann-Katherine Carton, GE-Healthcare, France

V1

Grenoble, September 2016

Contents

List of Figures

Chapter 1

Report

1.1 Abstract

The aim of this work is to develop a 3D biomechanical Finite Element (FE) breast model in order to analyze various breast compression strategies and their impact on image quality and radiation dose.

In this purpose a customized finite element mesh is generated from segmented breast MRI. Four types of tissues are highlighted in the segmented images: muscle, adipose tissue, glandular tissue and skin. All breast tissues are modelled as neo-Hookean materials. Large breast deformations are simulated using this FE model with ANSYS software.

A particular attention is granted to modelling the breast support matrix computed of the fascia membrane and coopers ligament. These structures are included in the finite element geometry and modelled as a different tissue type.

A physical correct modelling of the breast requires the knowledge of the stress-free breast configuration. Here, this reference shape (i.e. without any residual stress) is computed using an adapted prediction-correction iterative algorithm. The unloading procedure uses the breast configuration in prone and supine position in order to find a unique displacement vector field induced by gravitational forces.

Finally, the model is evaluated by comparing the estimated breast deformations under gravity load with the experimental ones measured in three body positions: prone, supine and oblique supine.

1.2 Introduction

Mammography is a specific type of breast imaging that uses low-dose X-rays to detect cancer in early stage. During the exam, the women breast is compressed between two plates until a nearly uniform breast thickness is obtained. This technique optimizes image quality, hence the tissue visualization and reduces the absorbed dose of ionizing photons. But breast compression is also often a source of discomfort and sometime pain for the patient during and after the exam. Though the mammography is the most effective breast cancer screening

method, the discomfort perceived during the exam could deter women from getting the test. Therefore, alternative techniques allowing reduced breast compression is of potential interest.

The aim of this work is to develop a 3D biomechanical Finite Element (FE) breast model in order to analyze various breast compression strategies and their impact on image quality and radiation dose. CatSim environment [ref1] is used to create artificial breast images from numerical phantoms and to compute the corresponding averaged glandular dose. The biomechanical model estimates the compressed phantom geometry relative to the applied forces before being introduced in the image simulation workflow. From the finite element solution, the 3D strain cartography is computed as a first guest of pain and discomfort.

1.2.1 Finite element breast models

Biomechanical modelling of breast tissues is finding a wide use in various medical applications such as surgical procedure training, pre-operative planning, diagnosis and clinical biopsy, image guided surgery and image registration, material parameter estimation. For the last 20 years several research groups have presented their breast models based on finite elements theory. One of the first breast biomechanical models based on the finite element theory is the one proposed by [Azar et al., 2002]. The model is used as a novel method for guiding clinical breast biopsy. The breast tissue is considered homogeneous, isotropic, incompressible, non-linear material. The compression is modelled using virtual compression plates by applying displacements to the surface nodes. Large deformation is approximated by a sum of small increments using small-strain considerations.

Later more complex models where developed implying different types of tissues, anisotropies, large deformation theory and more complex boundary conditions. [Rajagopal et al., 2004] developed a model based on large deformation mechanics in order to validate the assumption of isotropy, homogeneity and incompressibility of soft tissues. The material models where computed using the bibliography data only. The method was validated experimentally using silicone gel phantoms subjected to gravitational loading. [Rajagopal, 2007] also studied the effect of modelling the breast skin layer. And as [Pathmanathan et al., 2008] research team they found that modelling the skin result in an underestimation of breast displacements.

[Han et al., 2012] developed a bio-mechanical breast model for surgical simulations. In their model 3 types of tissues are considered: muscle, glandular and adipose tissues. [Gamage et al., 2012] introduced the pectoral muscle in the breast mechanical model and showed that the muscle should be accounted in the biomechanical breast modelling.

The anisotropic effect of Cooper's ligaments was introduced for the first time by [Pathmanathan et al., 2008] and took up again by [Han et al., 2012]. They have introduced an additional factor in the stress-strain energy function describing the transverse isotropic properties. They considered the breast heterogeneity by modelling adipose tissue and fibro-glandular tissues like different materials. However, the model was not validated using clinical data. A new modelling method for Cooper's ligaments vas proposed by [geo, 2016].

They added a generic ligaments model based on a mass-spring system to the finite element model.

The deformation of an elastic body is typically performed by specifying appropriate boundary conditions. Almost all biomechanical breast models are based on fixed boundary conditions, i.e. the nodes lying on the posterior face of the breast are defined with zero-displacement proprieties. [Carter et al., 2012] replaced the "fixed" boundary conditions by a "sliding" region between the posterior part of the breast and anterior part of the pectoral muscle. Recently the [Ptz, 2015] team have presented a new time-preserving method to model the sliding motion. The sliding method is based on fixed boundary conditions in conjugation with an explicit update computed using the resulting internal forces of the elastic material.

The bibliography present 3 main difficulties in the breast mechanical simulation:

1. Unknown stress-free breast configuration. Since, for all in-vivo studies, the breast geometry is extracted from the MRI data, the measured configuration represents the breast subjected to the gravity loading. Thus, for a Finite Element modeling it is very important to accurately predict the unloaded (i.e. stress-free) configuration.

2. Unknown elastic parameters of breast soft tissues. The bibliography shows a very large interval of elastic parameters depending of the experimental methods and made assumption.

3. Breast tissues are known to be extremely soft. Very large deformation of materials implies excessive elements distortion. A poor mesh quality can lead to inaccurate results and numerical instability. This problem was raised for the first time by [Kuhlmann et al., 2013]. To solve the large deformation problem, they proposed a coupled Eulerian-Lagrangian FE method. According to the authors this method is more relevant for breast soft tissues but is highly time-consuming.

1.2.2 Breast tissue biomecanical modeling

Global breast mechanics are governed by breast tissue compositions and their individual mechanical properties. Therefore, an accurate breast model stands on a good knowledge of breast anatomy and on good characterization of the mechanical behavior of the involved tissues.

Multiple studies have showed that female breast composition and so its mechanical behavior undergo substantial changes during the lifetime. The first studies on estimation of mechanical proprieties of breast tissues were done in diagnostic purposes. Presence of tissues with mechanical proprieties different from the breast-like tissues implies breast anomalies. The study published by [Krouskop et al., 1998] show the difference in stiffness between breast tissues and carcinomas. In this study authors supposed that the difference in breast global stiffness is due only to the changes in breast tissues compositions and not in changes of the individual material property. Therefore, they have studied ex-vivo 142 tissues samples from different subjects and they assumed their homogeneity. The samples

were representing 4 type of tissues: adipose tissue, glandular tissue, fibrous tissue and carcinoma. They showed that do to the difference in material stiffness measured using elastography they are able to detect pathological changes in breast tissues and moreover they can estimate elastic parameters of normal tissues images from elastography.

Later, several research groups have presented values of elastic modulus of adipose and glandular tissues. The range of elastic parameters is going from 0.1 kPa to 271.8 kPa (see table 1.1). Such big variation can be explained be the differences in the used methods but also by the different physical condition, age or period of the menstrual cycle of the participants. [LORENZEN et al., 2003] found that during the menstrual cycle, due to the hormonal changes, the elastic properties of the glandular tissues can change by about 30 %.

An important difference in the estimated elastic modulus of soft tissues is observed between the linear elastic and hyperelastic models. In the earlier studies where authors are using a hyperelastic Neo-Hookean models with in-vivo measurements, the range of the adipose and glandular elastic modulus is lower than 1kPa, compared to an average of 20-30 kPa given be the linear models with ex-vivo measurements.

[Carter, 2009b] used a Finite Element breast model considering 3 types of tissues: adipose tissue, glandular tissue and skin. All 3 tissues were modelled as Heo-Hookean incompressible materials. His model allows a better modeling of tissues in-vivo conditions, i.e. in-vivo tissues interaction. Since the soft tissues are of the same density as the water, the submerged in water breast was considered to have zero internal stress. The elastic parameters are estimated by minimizing the difference between computed and measured prone breast configurations. For this model the authors obtained elastic modulus equal to 0.2 kPa for adipose tissue, 0.4 kPa for glandular tissue and 10 kPa for skin.

[Gamage et al., 2012] have considered the breast as a homogeneous material but have also included the pectoral muscle in the biomechanical model. Both of tissues were modelled as hyperelastic materials. They obtained 0.1 kPa for elastic modulus of the homogeneous breast and 0.52 kPa for muscle.

[Van Houten et al., 2003] have considered also the Poisson Ration as an model variable. The estimation is done in in-vivo conditions (based in magnetic resonance elastography). The authors assume linear material behavior therefore the elastic modulus and Poisson Ration are computed from the 2 Lame modulus. They found that the Poisson Ration for adipose tissue lies between 0.34-0.4 and for glandular tissue around 0.4.

Previously listed researches clearly showed the variability of elastic modulus of the same tissue between and within individuals. [Eder et al., 2014] made a large analysis of all existing material models. According to their findings many of proposed in the literature parameters are too stiff, and namely those that are obtained by indentation ex-vivo test. The more reliable values are given by [Rajagopal et al., 2008], the other values permitting not enough deformation due to the gravity loading.

Ex-vivo estimation				
Author	Method	Material model	Material constants	
			Adipose	Glandular
[Krouskop et al., 1998] - 5% precomp.	identation	Linear elastic	E=20 kPa	E=33 kPa
[Krouskop et al., 1998] - 20% precomp.	identation	Linear elastic	E=20 kPa	E=57 kPa
[Wellman et al., 1999]- 5% precomp.	identation	Linear elastic	E=6.6 kPa	E=33 kPa
[Wellman et al., 1999]- 15% precomp.	identation	Linear elastic	E=17.4 kPa	E=271.8 kPa
[Samani, 2007]	identation	Linear elastic	E=3.25 kPa	E=3.24 kPa
In-vivo estimation				
[Van Houten et al., 2003]	MRE	Linear elastic	E=17-26 kPa	E=26-30 kPa
[Carter, 2009b]	MRI	Neo-Hookean	C_{10}=0.2-1 kPa	C_{10}=0.4-0.8 kPa
[Han et al., 2012]	MRI	Neo-Hookean	E=1 kPa	E=0.22-43.64 kPa
[Gamage et al., 2012]	MRI	Neo-Hookean	C_{10}=0.1 kPa	C_{10}=0.1 kPa
[Rajagopal et al., 2008]	MRI	Neo-Hookean	C_{10}=0.08 kPa	C_{10}=0.13 kPa

Table 1.1: Elastic modulus of adipose and glandular tissues

1.2.3 Skin biomechanical modeling

The skin mechanical parameters are also important in breast mechanics. Only [Carter, 2009b] have included the skin in the identification process of the breast soft tissues elastic modulus. The authors modeled the skin as a Neo-Hookean incompressible material, and they obtained an elastic modulus equal to $10kPa$.

[Sutradhar and Miller, 2013] published a complete study of breast skin estimating the thickness and elasticity for 16 different breast regions. The study was done on twenty-tress female volunteers aging from 29 to 75 ears. With in-vivo suction experiments they found an average thickness of $1.55mm$ and an elastic modulus of 334kPa. They also showed the regional variation of skin thickness: according to the authors the lateral region thickness is the thinnest among all the breast regions followed by superior/inferior part (without any significant differences) and the medial region. Concerning the radial distribution, the interior region closer to the nipple was more thin than the exterior radial part of the breast. A similar regional variation study was done on the skin elasticity. It was found no significant variation of elastic modulus in radial direction. The modulus was found grater in the superior and lateral part than in the inferior and medial parts respectively. An additional measurement was done in order to compare the skin elastic modulus in supine and upright position with no significant differences found.

Other research on skin elasticity are available, but they are not specific to the breast skin. [Hendriks et al., 2006] estimated in-vivo skin proprieties by suction testing. The skin was considered as a homogeneous,isotropic, incompressible, hyperelastic material. The study was performed on 14 subjects and the obtained average of elastic modulus for skin was $58,4kPa$.

1.2.4 Stress-free breast configuration

As mentioned before, in the breast configuration given by MRI images the soft tissues are pre-stressed due to in-vivo conditions (i.e gravitational forces). In order to apply the continuum mechanics theory, an initial stress-free breast shape is needed.

One of the existing methods is the backward finite element formulation used by [Pathmanathan, 2006] in his biomechanical model. The method is based in the reformulation of the virtual work equation, where the residual forces are expressed in terms of unknown reference state coordinates.

[Carter, 2009a] addressed the same problem solving an iterative sequence of forward deformations where the only unknown is the reference configuration. First, the reference configuration is assumed to be equal to the prone breast configuration. Second the gravity loading is applied in order to compute a first estimation of the prone configuration. From the first estimation of deformed state a difference in node location is computed. Then, the reference state is perturbed accordingly to the computed difference until convergence is achieved.

Later [Eiben et al., 2014] refined the method by translating the difference location vector from the deformed space to the reference space by multiplying the vector with the

invers deformation gradient. [Eiben et al., 2014] compared the two previous methods, according to the authors the backward formulation methods exhibits excellent results only then elastic parameters are well known. Since in the prone-supine breast deformation context the elastic parameters are unknown, there is no significant numerical difference between the two methods.

1.3 Materials and methods

1.3.1 Breast Anatomy

A good knowledge of anatomical breast structure and its composition is necessary then one is developing a biomechanical breast model. The tissues distribution and their biomechanical properties define the global breast mechanics.

The woman breast main function is to produce, store and release milk for baby feeding. Anatomically, the adult breast sits atop the ribcage. The breast tissue extends horizontally (side-to-side) from the edge of the sternum out to the midaxillary line. Its heterogeneous structure is composed of glandular, fatty and connective tissue (see fig. 1.1).

Skin

The skin is the covering breast layer which provides protection and receives sensory stimuli from the external environment. It is a heterogeneous organ composed of 3 layers: epidermis, dermis and hypodermis.

Fatty tissue.

Fatty tissue is the predominant tissue of the breast that fills up depressions between the two layers of fascia. The aim of this tissue is to surround and protect the lobes and the ducts. The amount of fat determines the size of the breast.

Glandular tissue.

Glandular tissue is represented by breast lobes. A healthy female breast is made up of 12-20 lobes which are responsible for milk production. Mammary ducts arise from these milk sources as branches and connect them to the female nipple. There are about 10 duct system in each breast that carry the milk from the lobes to the nipple. The dark area of skin surrounding the nipple is called the areola.

Connective tissue.

Connective tissue is computed of the Cooper's ligaments and fascial system. Fascia mammae is divided into a superficial and a deep layer. Cooper's ligaments run from the super-

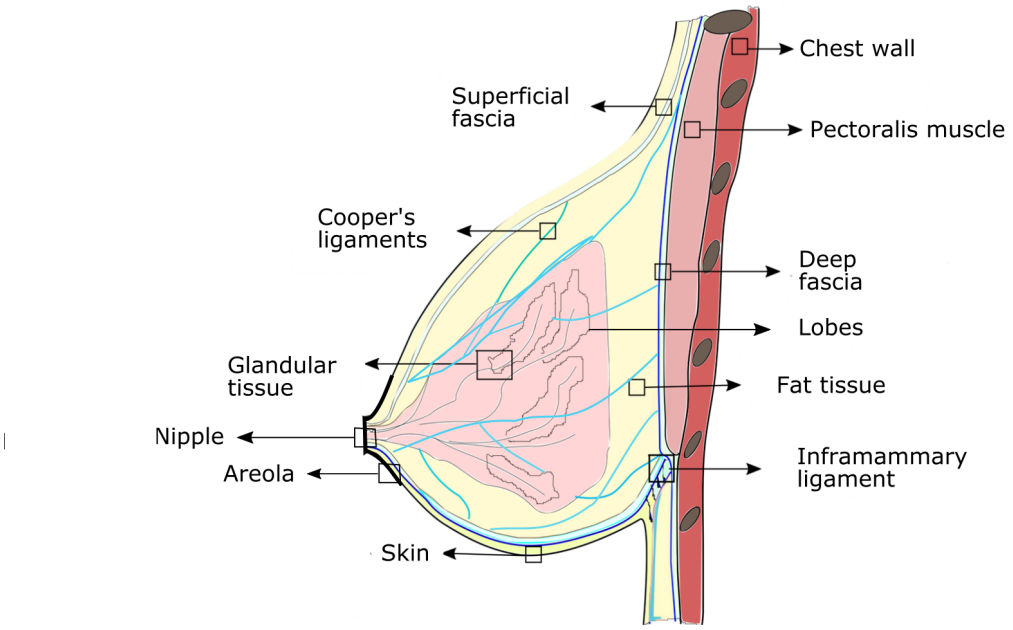

Figure 1.1: Breast anatomy

ficial fascia through the breast and attach to deep fascia (see Fig. 1.1). The intersection of the two fascias in the region of the 5th and 6th rib forms the inframammary crease ligament. These ligaments extend all around the breast to form a stiff 3D structure fixing the breast tissues to the chest wall. The connective tissue provides support to the breast and gives it its shape.

Breast texture changes

The female breast undergoes substantial changes during the lifetime. The main part of them is caused by hormones and by woman's physiological condition. Important changes in female breast stiffness and composition occur during the menstrual cycle, pregnancy and menopause.

The work by **Lorenzen et all** showed that during the premenstrual phase of menstrual cycle the stiffness of fibro-glandular tissue and glandular tissue can change be 30% and 14 % respectively. They also show that in middle of menstrual cycle the parenchyma volume increases of 38% and the water content by 24.5%. As the breast content shows a variability between and within subjects, an accurate breast biomechanical model must take into consideration the subject specific variations.

1.3.2 Volunteers and MRI acquisition

The MRI image data are acquired in order to compute and validate the biomechanical model. All volunteers have agreed to participate in this experiment within a pilot study

approved by an ethics committee. The computed data base contains breast images of three volunteers within 45 years old with various breast dimensions. Three different positioning configurations are considered for each volunteer (see fig 1.2): prone, supine and supine titled.

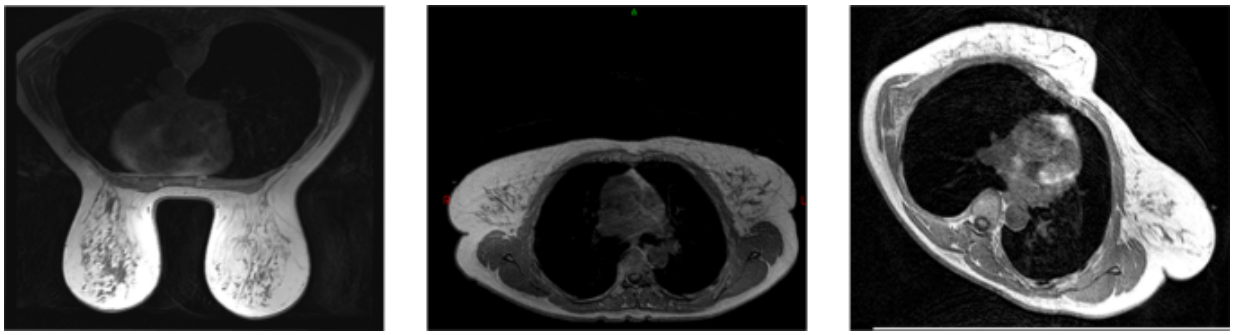

Figure 1.2: Three breast configuration under gravity loads: a) prone position; b) supine position c) supine tilted.

Before the image acquisition, each volunteer was asked to fix 10 fiducials markers on the chest and the surface of the breast as showed in fig 1.3. The first four markers are placed on the fixed part of the chest in order to define a rigid body reference system. This set of markers will be used to compute the rigid transformation between 2 different body positions. The last six marchers are placed to track the breast mechanics and will be used to estimate the model accuracy. During the image acquisition, it was verified that the breast is not in contact with any other objects or body's parts.

The images were acquired with a Siemens 3T MRI scanner using T2 weighted image sequence. The image resolution in plane is of 0.5x0.5 mm and 0.6 slice thickness.

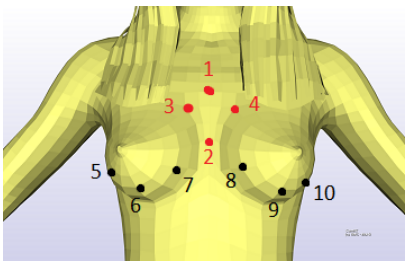

Figure 1.3: Graphycal fiducial markers position on the woman chest.

1.3.3 Image prepossessing

During the imaging process the volunteers are going in and out of the MRI scanner. Therefore, the breast undergoes not only elastic transformation but also a rigid one. Simulation of breast deformation under gravity loading assumes that the breast support (rib cage) is fixed and the breast displacement is due to gravitational forces only. In order to meet the simulation conditions, the breast rigid transformation is computed using image registration methods.

Next the MRI images are used to generate the patient specific finite element mesh. In this purpose the images are segmented in order to differentiate 4 types of tissues: glandular tissue, adipose tissue, pectoral muscle and skin.

Image registration

The image registration is performed considering a rigid body transformation: rotation and translation of the body inside the MRI scanner. During the body re-positioning the breast fulfil an elastic transformation. Excluding the soft tissues from the registration process will increase considerably the results accuracy. Thus, for the registration processes the image field of view is reduced to the rib cage only.

The image registration process is performed in 2 steps

1. An initial rigid transform is computed by registering the 4 points corresponding to the 4 reference markers (fiducial markers 1-4 in fig 1.3). The transformation is estimated using the iterative closes point (ICP) algorithm minimizing the mean Euclidean distance between the 4 points.

2. A second optimization process is performed based on the image grey intensity using gradient descent method. This time the metric function is computed using the normalized cross-correlation function. At the first iteration of the optimization process the transformation is initialized with the results from the first step.

The final transform is applied to the whole image such that the breast will follow the movement of the rib cage.

Image segmentation

The image segmentation was performed using semi-automated active contour method implemented in ITK-snap software. First the breast tissues and pectoral muscle masks were computed from the whole image, second the breast tissues are divided in glandular and adipose tissue (see fig. 1.5).

The segmentation process for one tissue type take place in 3 steps (see fig 1.4):

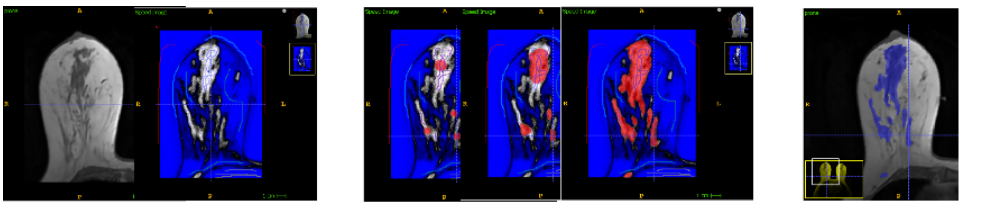

Figure 1.4: Example of tissues segmentation: glandular tissue .

1. Computation of the speed image: the speed image is a new synthetic image with values in the range of -1 and 1. The values of 1 represent the segmented tissue and -1 the background. A random forest learning algorithm is used in order to compute the probability that a pixel belong to the defined class. The training features are selected such that the state and space characteristics are included.

2. Initialization: One or more seeds point is placed in the region of interests. These points will be grown to form the segmented structure in the next step.

3. Region growing: evolution of the placed seeds. The placed point will evaluate on time according to the speed images: expending on the positive regions, contracting over the negatives ones

1.3.4 Subject-specific Finite Element mesh generation

Subject specific Finite Element (FE) mesh is computed using Bolt software.

First a homogeneous hexa-dominant mesh is generated from the stl volumes (breast + muscle). Next, form each finite element a material type is assigned by spatial identification with the segmented data. The tissue type assigned to an element is the tissue with a maximal number of pixels inside the element's convex envelope. At this step the finite element mesh is composed of 3 type of materials: pectoral muscle, adipose tissue, glandular tissue. Finally, two hexahedral layers are added: one of 0.1 mm and the second one of 2 mm (see fig. 1.5). These layers will represent the fascia and the skin layer respectively.

1.3.5 Biomechanical soft tissues model

The large deformation of breast soft tissues was modelled using finite strain formulation of the finite element method from the ANSYS commercial package. In our model we will

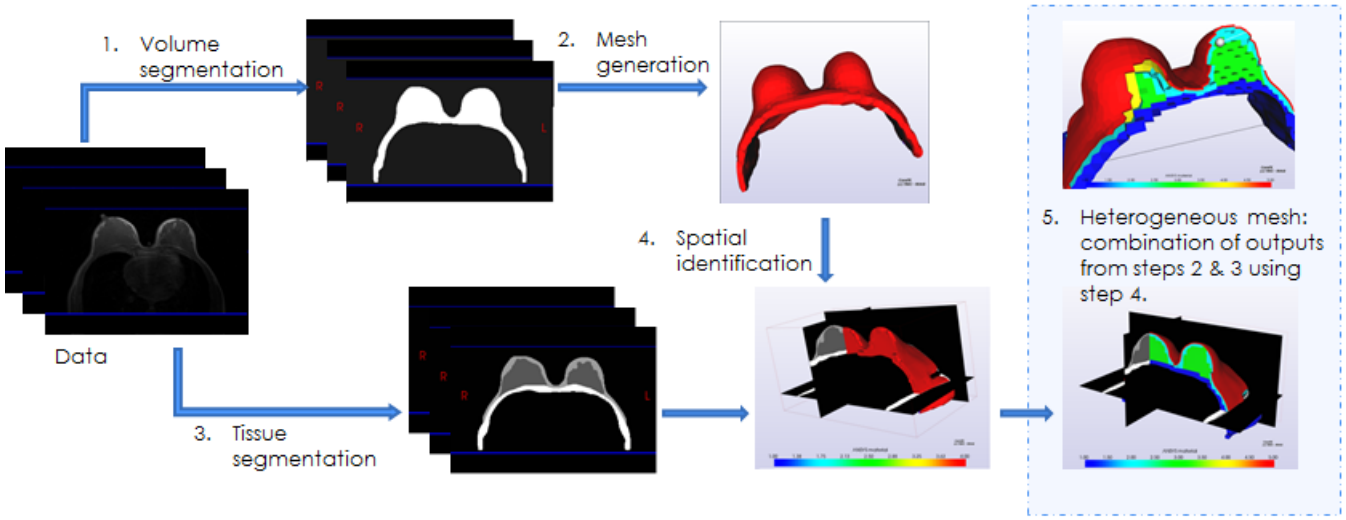

Figure 1.5: Subject-specific heterogeneous mesh generation.

consider 5 types of tissues: pectoral muscle, adipose tissue, glandular tissue, superficial fascia and skin. In reality, the breast tissues are: anisotropic due to the Coopers ligament reinforcing the breast in the muscle-to-skin direction; quasi-incompressible due to the presence of lactiferous ducts and blood vessels; heterogeneous and hyperelastic. Here, the breast soft tissues will be modelled as homogeneous, isotropic, quasi-incompressible and hyperelastic models. To model the mechanical response of breast tissue we are using a Neo-Hookean model with the strain-energy potential:

$$W = \frac{\mu}{2}(I_1 - 3) + \frac{k}{2}(J-1)^2$$

Here μ is the initial shear modulus, k is Bulk modulus, I_1 first invariant of Cauchy stress tensor and J the volume ratio. The material parameters μ and k can be determined form Young's modulus E and Poisson ratio υ through the relations:

$$\mu = \frac{E}{2(1+\upsilon)} \quad k = \frac{E}{3(1-2\upsilon)}$$

The Young's modulus and Poisson ratio are defined for each material separately.

1.3.6 Boundary conditions

The bibliography presents two type of boundary conditions (see appendix A.1): zero-displacement nodes defined on the surface between the breast and the pectoral muscle and sliding surfaces between the breast and pectoral muscle. As we include the pectoral muscle in the model, we use zero-displacement conditions for the nodes of its posterior surface. The muscle and the breast tissues are perfectly sticked together by sharing the

same nodes on the intersection surface. The skin and fascia layer is extending up to the pectoral muscle in order to limit the soft tissues deformation in the region of axilla ends, shoulder and inferior part of rib cage.

1.3.7 Estimating the stress-free breast configuration

As mentioned before, the estimation of the stress-free breast configuration it's very important part of breast biomechanical simulations. The methods based on a patient specific finite element mesh need a estimation of the pre-constraints due to the gravity loading. Our method is based on the one proposed by [Carter, 2009a] and adapted later by [Eiben et al., 2014] and [Eder et al., 2014].

The original method is represented in fig. 1.6. The process begins by considering that the experimental deformed geometry DG_{exp} have zero internal stress. Then, the gravity is applied in the reverse direction which gives a first estimation of initial stress-free state (reference state) RG_0. Next, the gravity is reloaded in the natural direction and the guess of the deformed state is given DG_{guess}. At this step the node's spatial location is compared between the estimated deformed state and the measured one. The difference of node location is applied on the reference state RG_i. The process is repeated until the convergence is achieved.

Here, the same iterative process is used but with a different initialization of the initial stress-free geometry RG_0 and different update computation δ_{nodes}.

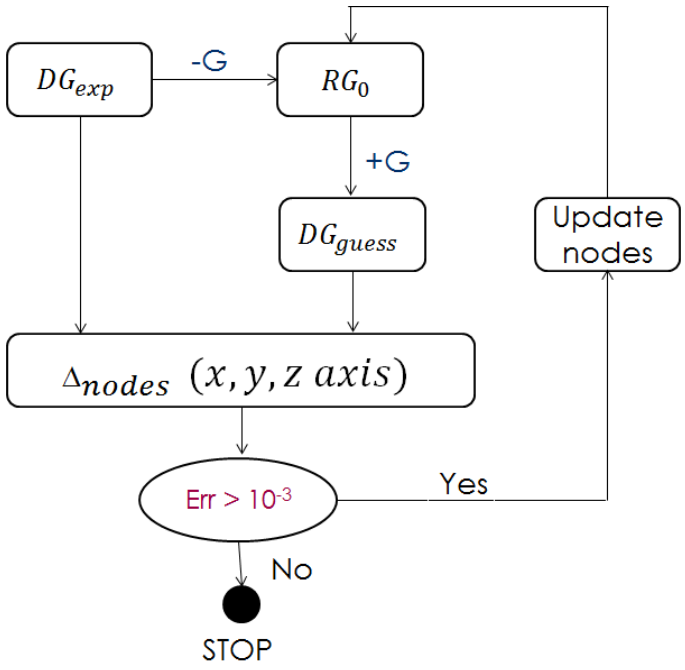

Figure 1.6: Iterative scheme for stress-free geometry estimation.

First guess of stress-free geometry

The first estimation of the stress-free geometry is very important for the method accuracy and convergence. Generally, the iterative optimization methods are dependent on their initialization. If initialization is not situated in the solution's neighborhood the optimization can be stuck in a local extrema or have problems to achieve the convergence. As we dispose of two opposite breast deformed geometries (supine and prone position) we combined them in order to compute an "intermediary geometry" which will be used as initialization of the optimization process. The combination of the two geometries is purely geometrical and has no biomechanical meaning.

First, an elastic mesh registration method is applied to match the supine geometry to the prone geometry. The mesh registration algorithm used was developed by [Bucki et al., 2010] for a fast and automated mesh generation method. The algorithm computes an elastic transformation from a source mesh to a target mesh preserving the elements regularity. The transformation is computed using the surface nodes only but is valid for the entire deformation space. A regularization strategy limits excessive space distortions. In this context we can translate the supine finite element mesh in the prone configuration without element distortions. From the two configuration of the same finite element mesh, now we are able to compute the mean between node's locations. Finally, our initialization geometry is computed by the finite element mesh having each node at the mean location between the prone and supine configuration.

Update computation

In the previous versions of the iterative algorithm the update calculation for the initial state is computed for each node of the finite element mesh. The finite element mesh used in our simulations is composed by elements of mean edge length of $4mm$. An excessively big number of nodes mean too many conditions for the optimization problem. Thus, the geometry optimization is hyper-constrained and the convergence is achieved to fast without finding the solution. To avoid this problem, we propose a different estimation of the geometry update. In this scope, instead to use all mesh nodes for the update estimation, we will compute an elastic transformation to map the surface nodes from source mesh to the target mesh.

As proposed by [Carter, 2009a], from the estimated stress-free configuration an estimation of the deformed geometry is computed by applying the gravitational forces in their natural direction: forward to simulate the prone position or backward to simulate the supine position. Then, using the mesh registration algorithm an elastic transformation is computed to map the surface nodes of estimated deformed geometry to the surface of the real deformed configuration. Then, the computed transformation is applied on the stress-free geometry. The process is repeated until the convergence is achieved.

1.4 Results and Discussions

1.4.1 Breast soft tissue elastic parameters.

The values of the soft tissues presented in the literature goes from 0.1 kPa to 57kPa. The purpose of this experiment is to investigate the model sensibility to the tissue elasticity and to find a smaller interval for the elastic modulus. In order to evaluate the impact of the tissues elasticity on the breast mechanics we have made several basic simulations. For the first test we assumed that the skin, the glandular and adipose tissues are described by the same Neo-Hookean low. The Poisson ration of the pectoral muscle and the breast soft tissues was fixed at 0.45. The elastic modulus of the pectoral muscle was fixed at $30kPa$ and for the breast soft tissues was set to $0.5kPa$, $1kPa$, $5kPa$, $10kPa$ et $20kPa$ consecutively.

The simulation process is divided in 2 steps. First, we consider the supine configuration with zero-internal forces and then we apply the reverse gravity. The new estimation is supposed to by the "stress-free" breast configuration. Next, the gravity is applied in the forward direction in order to estimate the prone breast configuration. From the estimated prone breast geometry, the 3D location of the nipple is registered and compared to the nipple position in the experimental prone position. Table 1.2 shows the Euclidean distance between nipple location in the estimated geometry and the one in experimental obtained geometry. We observe that an elastic modulus of $20kPa$ for breast is too stiff, the maximal node displacement is equal to $2.23mm$ which is too small to describe the the breast mechanics from supine to prone configuration.

Side	D (mm) E=0.5kPa	D (mm) E=1kPa	D (mm) E=5kPa	D (mm) E=10kPa	D (mm) E=20kPa	supine
Left	17.00	29.32	37.17	38.05	38.80	39.11
Right	6.62	25.94	37.43	38.72	39.88	39.89
Max Disp.	23.30	9.12	3.21	2.66	2.23	

Table 1.2: Nipple location error computed between estimated and experimental loaded prone breast position. D= euclidean distance from estimated location to experimental location. Max Disp = maximal nodal displacement for corresponding elastic modulus. Supine = euclidean distance of nipple location between supine and prone position

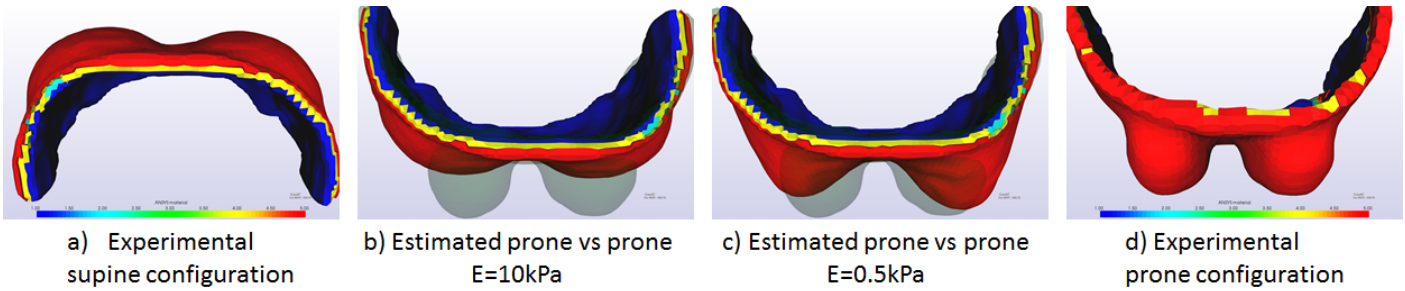

Figure 1.7: Breast deformation depending on elastic modulus.

According to the obtained results, we can conclude that the elastic modulus of breast soft tissues is more likely to by around 1 kPa. Most of the values given in the literature underestimate the breast deformation (see fig. 1.7). Same results have been obtained by [Carter, 2009b, Han et al., 2012, Rajagopal et al., 2008] using a similar FE method. But their results dose note describes the intra-subject elasticity variation. We have seen the elastic properties for one subject can change for about 30% within a moth ([LORENZEN et al., 2003]), our results show that the biomechanical breast model is very sensible to the tissues elastic modulus, therefore, it is very important to have a good approximation of the elastic parameters.

Our model included only adipose tissues, it must be mentioned that the glandular tissue and human skin are stiffer than the adipose tissue. Thus we must consider that adding this tissues in the model will rigidify the entire structure.

A optimization methods of elastic parameters such as the one presented by [Carter, 2009b] must to be developed in order to estimate them for each subject and for each type of tissue.

1.4.2 Skin impact in breast mechanics.

The skin is covering the breast tissues like en elastic envelope. As it is stiffer than the breast soft tissues, the skin mechanical properties govern the global breast mechanics. In this section we discuss the influence of the skin layer on breast mechanics caused by gravity loading.

In this scope, we have done simulation using 2 breast models. The first one is computed from 3 type of materials: muscles, breast soft tissues (glandular + adipose) and skin. The second one contains only muscle and breast tissues. All tissues are quasi-incompressible Heo-Hookean materials. According to the literature and to our previous results we chose the elastic parameters for skin, breast and muscle equal to $10kPa$, $1kPa$ and $30kPa$ respectively. For this section we consider the prone configuration as the "stress-free" one (i.e zero internal stress) and we simulate the up-right breast configuration with and without the skin layer.

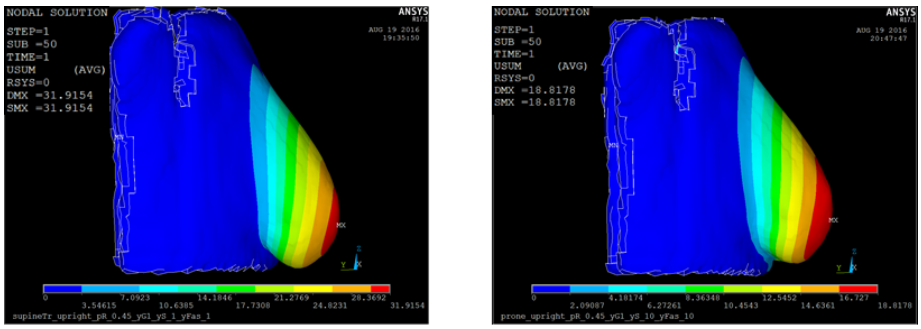

a) Upright position homogeneous breast

a) Upright position Homogeneous breast + skin

Figure 1.8: Upright breast configuration with and without skin layer.

Figure 1.8 show the difference between the upright position computed with and without skin layer. The skin layer can reduce the breast nodal displacement up to 30%. the advantage of considering the skin in breast deformation simulations are the changes in breast shape which is closer to the natural breast shape in upright position.

1.4.3 Stress-free configuration estimation.

The estimation of the stress-free configuration is a big challenge in breast biomechanical modeling. As we assume that the breast tissues are non-linear material, a simple reverse gravity method is not relevant. Thus we implemented the iterative scheme from [Carter, 2009b] in order to estimate the reference geometry. The model contains 3 types of tissues as hyperelastic model with elastic modulus equal to $10kPa$, $1kPa$ and $30kPa$ for skin, breast and muscle respectively.

As we can see in fig.1.9 (second line) the estimated stress-free configuration is too close to the experimental supine configuration. The reason of the poor approximation is the assumption of zero internal stress in supine position at first iteration and also non adapted elastic parameters. Firstly, the chosen elastic materials turn the breast in a too stiff structure, therefore the large deformations are not achieved. Secondly, the optimization algorithm is initialized with the supine geometry with the assumption of zero internal stress, the breast geometry being too far from the reference one, the algorithm can be stoked in a local minimum.

Introducing the new stress-free geometry (fig 1.9 first line, second column) which represents only the first approximation of the stress-free configuration, i.e. without applying any iterative algorithm, the results are improved. The estimated breast geometry in prone position is closer to the experimental data. The difference between the 2 geometries can be

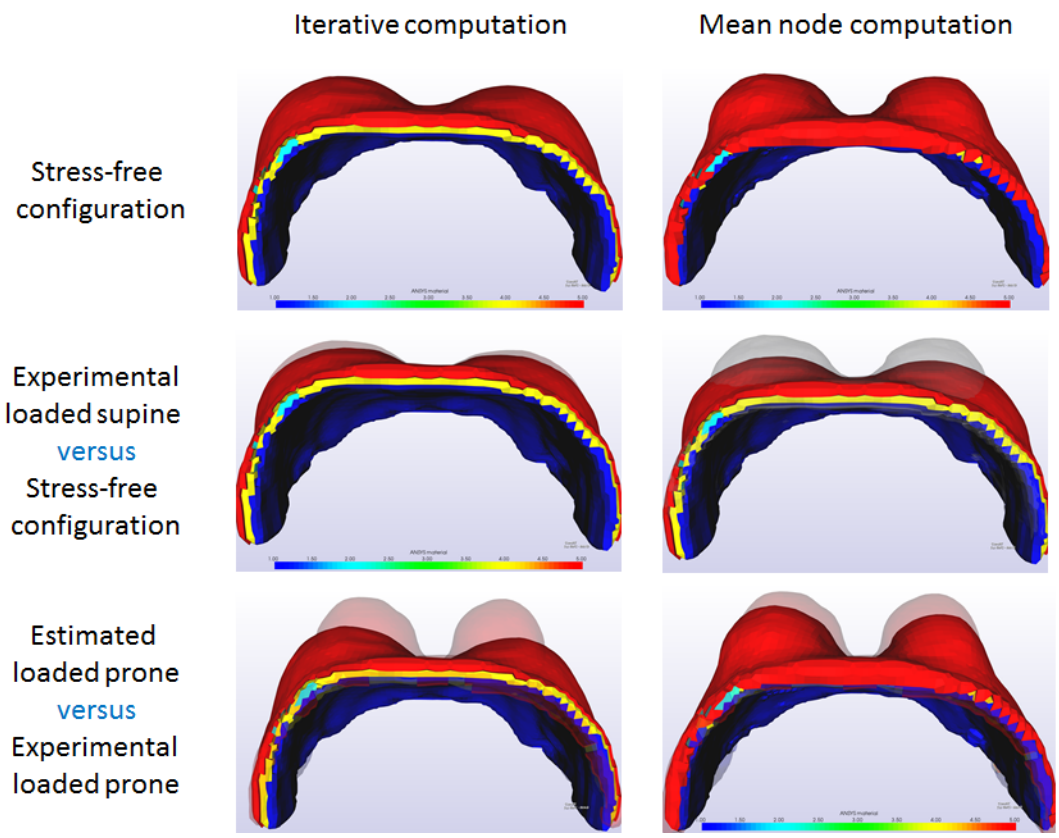

Figure 1.9: Zero-stress geometry estimation results.

improved by optimizing the materials elastic parameters. By taking the elastic modulus for breast and skin equals to $0.3kPa$ and $10kPa$ ([Carter, 2009b]) the estimated supine and prone configuration are considerably improved. Fig 1.10 shows the obtained results for loaded breast geometry in supine and prone positions compared to the experimental obtained geometry in supine and prone positions.

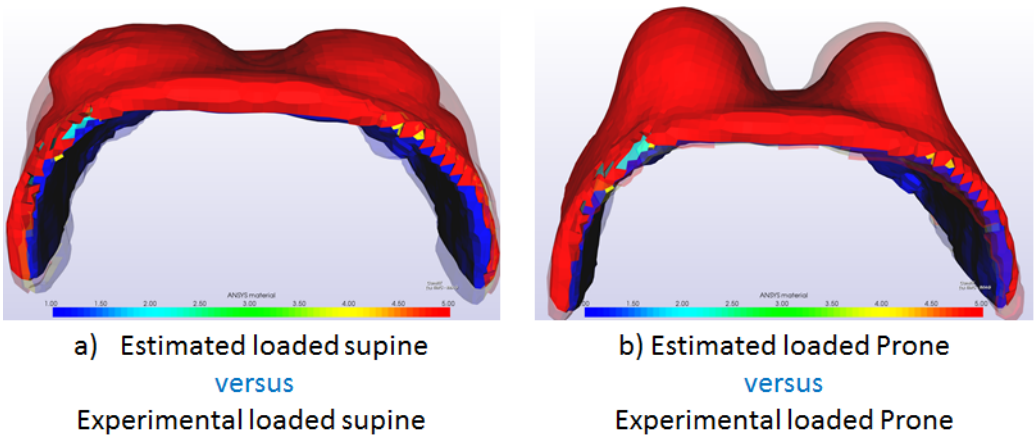

Figure 1.10: Estimated prone and supine configurations versus experimental measures. Elastic parameters: muscle= 30kPa, breast=0.3 kPa, skin= 10kPa

1.5 Conclusion

Modeling breast deformations is a challenging problem due to its anatomical complexity. First of all, the breast tissues are extremely soft and the elastic parameters variate depending not only on the subject but also on their physical and physiological condition. As we have seen the biomechanical model is very sensible to the elastic modulus, thus their estimation is indispensable for every new subject.

An the over hand, the deformations that are usually applied to breast tissues, either gravity loading or paddle compression, are considerable do to a low elastic modulus. Thus, they imply excessive elements distortions and respectively inaccurate results and numerical instability. It is difficult to emphasize an optimization algorithm on poor quality finite element mesh, because it will have numerical problems before achieving the convergence. This problem has been treated by [Kuhlmann et al., 2013] by combining the Eulerian and Lagrangian material formulations. According to the authors, the Eulerian formulation describes better the large deformations that adipose and glandular tissues are subjected.

Finally, the third important difficulty in breast mechanics modeling is the unknown "stress-free" configuration. Which in in-vivo conditions, cause to the gravity, is not easy to obtain with experimental measurements.

We plan to compute the patient specific elastic parameters by implementing an optimization algorithm. The method will give the elastic parameters with the beast match between supine and prone positions. Concerning the stress-free configuration, we plan to improve it bay matching our first approximation with the prone or supine position. We will use the fixed point iterative algorithm with the new node location updates.

The difficulties that we found in implementation of both methods is the poor elements quality of the finite element mesh. Even if we start with a high- quality mesh, after one iteration the elements are distorted and no further iterations are possible. In order to solve this problem, we plan to include in the simulation workflow a re-meshing step in order to

control the elements quality with big deformations.

Bibliography

[geo, 2016] (2016). Simulation and Visualization to Support Breast Surgery Planning. volume 9699 of *Lecture Notes in Computer Science*, Cham. Springer International Publishing. 2, 26

[Azar et al., 2002] Azar, F. S., Metaxas, D. N., and Schnall, M. D. (2002). Methods for modeling and predicting mechanical deformations of the breast under external perturbations. *Medical Image Analysis*, 6(1):1–27. 2, 26

[Bucki et al., 2010] Bucki, M., Lobos, C., and Payan, Y. (2010). A fast and robust patient specific Finite Element mesh registration technique: Application to 60 clinical cases. *Medical Image Analysis*, 14(3):303–317. 14

[Carter, 2009a] Carter, T. (2009a). *Biomechanical modelling of the breast for image-guided surgery*. PhD thesis. 6, 13, 14

[Carter et al., 2012] Carter, T., Han, L., Taylor, Z., Tanner, C., Beechy-Newman, N., Ourselin, S., and Hawkes, D. (2012). Application of Biomechanical Modelling to Image-Guided Breast Surgery. In Payan, Y., editor, *Soft Tissue Biomechanical Modeling for Computer Assisted Surgery*, volume 11, pages 71–94. Springer Berlin Heidelberg, Berlin, Heidelberg. 3, 26

[Carter, 2009b] Carter, T. J. (2009b). Determining material properties of the breast for image-guided surgery. 4, 5, 6, 16, 17, 18

[Eder et al., 2014] Eder, M., Raith, S., Jalali, J., Volf, A., Settles, M., Machens, H.-G., and Kovacs, L. (2014). Comparison of Different Material Models to Simulate 3-D Breast Deformations Using Finite Element Analysis. *Annals of Biomedical Engineering*, 42(4):843–857. 4, 13

[Eiben et al., 2014] Eiben, B., Vavourakis, V., Hipwell, J. H., Kabus, S., Lorenz, C., Buelow, T., and Hawkes, D. J. (2014). Breast deformation modelling: comparison of methods to obtain a patient specific unloaded configuration. page 903615. 6, 7, 13

[Gamage et al., 2012] Gamage, T. P. B., Boyes, R., Rajagopal, V., Nielsen, P. M. F., and Nash, M. P. (2012). Modelling Prone to Supine Breast Deformation Under Gravity Loading Using Heterogeneous Finite Element Models. In Nielsen, P. M., Wittek, A., and

Miller, K., editors, *Computational Biomechanics for Medicine*, pages 29–38. Springer New York, New York, NY. 2, 4, 5, 26

[Han et al., 2012] Han, L., Hipwell, J. H., Tanner, C., Taylor, Z., Mertzanidou, T., Cardoso, J., Ourselin, S., and Hawkes, D. J. (2012). Development of patient-specific biomechanical models for predicting large breast deformation. *Physics in Medicine and Biology*, 57(2):455–472. 2, 5, 16, 26

[Hendriks et al., 2006] Hendriks, F., Brokken, D., Oomens, C., Bader, D., and Baaijens, F. (2006). The relative contributions of different skin layers to the mechanical behavior of human skin in vivo using suction experiments. *Medical Engineering & Physics*, 28(3):259–266. 6

[Krouskop et al., 1998] Krouskop, T. A., Wheeler, T. M., Kallel, F., Garra, B. S., and Hall, T. (1998). Elastic Moduli of Breast and Prostate Tissues under Compression. *Ultrasonic Imaging*, 20(4):260–274. 3, 5

[Kuhlmann et al., 2013] Kuhlmann, M., Fear, E., Ramirez-Serrano, A., and Federico, S. (2013). Mechanical model of the breast for the prediction of deformation during imaging. *Medical Engineering & Physics*, 35(4):470–478. 3, 19, 26

[LORENZEN et al., 2003] LORENZEN, J., Sinkus, R., Biesterfeldt, M., and Adam, G. (2003). Menstrual-cycle dependence of breast parenchyma elasticity: estimation with magnetic resonance elastography of breast tissue during the menstrual cycle. *Investigative radiology*, 38(4):236–240. 4, 16

[Patete et al., 2013] Patete, P., Iacono, M. I., Spadea, M. F., Trecate, G., Vergnaghi, D., Mainardi, L. T., and Baroni, G. (2013). A multi-tissue mass-spring model for computer assisted breast surgery. *Medical Engineering & Physics*, 35(1):47–53. 26

[Pathmanathan, 2006] Pathmanathan, P. (2006). *Predicting tumour location by simulating the deformation of the breast using nonlinear elasticity and the FEM*. PhD thesis. 6

[Pathmanathan et al., 2008] Pathmanathan, P., Gavaghan, D., Whiteley, J., Chapman, S., and Brady, J. (2008). Predicting Tumor Location by Modeling the Deformation of the Breast. *IEEE Transactions on Biomedical Engineering*, 55(10):2471–2480. 2, 26

[Ptz, 2015] Ptz, T. (2015). Sliding Motion in Breast Deformation Modeling. 3

[Rajagopal, 2007] Rajagopal, V. (2007). *Modelling breast tissue mechanics under gravity loading*. PhD thesis, Citeseer. 2, 26

[Rajagopal et al., 2008] Rajagopal, V., Lee, A., Chung, J.-H., Warren, R., Highnam, R. P., Nash, M. P., and Nielsen, P. M. (2008). Creating Individual-specific Biomechanical Models of the Breast for Medical Image Analysis. *Academic Radiology*, 15(11):1425–1436. 4, 5, 16

[Rajagopal et al., 2004] Rajagopal, V., Nielsen, P. M. F., and Nash, M. P. (2004). Development of a three-dimensional finite element model of breast mechanics. In *Engineering in Medicine and Biology Society, 2004. IEMBS'04. 26th Annual International Conference of the IEEE*, volume 2, pages 5080–5083. IEEE. 2, 26

[Samani, 2007] Samani, A. (2007). Elastic moduli of normal and pathological human breast tissues: an inversion-technique-based investigation of 169 samples. 5

[Sutradhar and Miller, 2013] Sutradhar, A. and Miller, M. J. (2013). *In vivo* measurement of breast skin elasticity and breast skin thickness. *Skin Research and Technology*, 19(1):e191–e199. 6

[Van Houten et al., 2003] Van Houten, E. E., Doyley, M. M., Kennedy, F. E., Weaver, J. B., and Paulsen, K. D. (2003). Initial in vivo experience with steady-state subzone-based MR elastography of the human breast. *Journal of Magnetic Resonance Imaging*, 17(1):72–85. 4, 5

[Wellman et al., 1999] Wellman, P., Howe, R. D., Dalton, E., and Kern, K. A. (1999). Breast tissue stiffness in compression is correlated to histological diagnosis. *Harvard BioRobotics Laboratory Technical Report*, pages 1–15. 5

Appendix A

Biomechanical breast models

Authors	Application	Computational Technique	Material models	Boundary conditions	Stress-free breast configuration
[Azar et al., 2002]	Image guided surgery	Small strain,continuum mechanics, FEM	skin-elastic linear, adipose,glamdular-hyperelastic polynomial	sliding (breast on the rib cage), contact regions (with lateral plates)	NA
[Rajagopal et al., 2004, Rajagopal, 2007],	Breast compression	Finite strain, continuum mechanics, FEM	Homogeneous , Neo-Hookean model	Zero-displacement BC	images of breast submerged in water
[Pathmanathan et al., 2008]	Image registration	Finite strain, continuum mechanics, FEM	Adipose, glandular, skin - hyperelastic materials; Cooper's ligaments-traversal isotropy factor	Zero-displacement BC	Backward analysis
[Han et al., 2012]	Surgical simulations	Finite strain, continuum mechanics, FEM	Muscle, glamdular, adipose-hyperelastic materials;Cooper's ligaments-traversal isotropy factor	Zero-displacement: anterior-posterior direction (z-axis) for pectoral muscle, y-axis direction muscle surface	NA
[Gamage et al., 2012]	Image guided surgery	Finite strain, continuum mechanics, FEM	homogeneous+ muscle- hyperelastic ideally incompressible materials	zero-displacement BC on rib cage surface, sternum, axilla ends, shoulder	inverse gravity (forward formulation)
[Patete et al., 2013]	Computer assisted breast surgery	Small strain,mass-spring	Adipose , glandular, skin	Zero-displacement BC on the chest wall	NA
[Kuhlmann et al., 2013]	Predict soft tissue deformation during imaging	Finite strain, continuum mechanics, FEM	Adipose, glandular- linear gel-like (Eulerian formulation); skin-quasi-incompressible isotropic hyperelastic material (Lagrangian formulation)	Zero-displacement chest wall	iterative scheme, incremental gravitational acceleration
[Carter et al., 2012]	MR-guided surgery	Finite strain, continuum mechanics, FEM	Homogeneous , Neo-Hookean model	sliding surface	Iterative scheme(forward problem, position update)
[geo, 2016]	Surgery simulation	Finite strain, continuum mechanics, FEM	homogeneous elastic material, Cooper's ligaments-generic mass-spring model	sliding BC (breast on the pectoral muscle)	NA

Table A.1: Breast biomechanical models